

## Structure-based design of cycloamide–urethane-derived novel inhibitors of human brain memapsin 2 ( $\beta$ -secretase)

Arun K. Ghosh,<sup>a,\*</sup> Thippeswamy Devasamudram,<sup>a,b</sup> Lin Hong,<sup>b,c</sup>  
Christopher DeZutter,<sup>a</sup> Xiaoming Xu,<sup>a</sup> Vajira Weerasena,<sup>b</sup> Gerald Koelsch,<sup>b,c</sup>  
Geoffrey Bilcer<sup>a,b</sup> and Jordan Tang<sup>c,d</sup>

<sup>a</sup>Department of Chemistry, University of Illinois at Chicago, 845 West Taylor Street, Chicago, IL 60607, USA

<sup>b</sup>Zapaq Inc., 755 Research Parkway, Oklahoma City, OK 73104, USA

<sup>c</sup>Protein Studies Program, Oklahoma Medical Research Foundation, University of Oklahoma Health Science Center, Oklahoma City, OK 73104, USA

<sup>d</sup>Department of Biochemistry and Molecular Biology, University of Oklahoma Health Science Center, Oklahoma City, OK 73104, USA

Received 17 September 2004; revised 27 October 2004; accepted 28 October 2004

Available online 21 November 2004

**Abstract**—A series of novel macrocyclic amide-urethanes was designed and synthesized based upon the X-ray crystal structure of our lead inhibitor (**1**, OM99-2 with eight residues) bound to memapsin 2. Ring size and substituent effects have been investigated. Cycloamide–urethanes containing 14- to 16-membered rings exhibited low nanomolar inhibitory potencies against human brain memapsin 2 ( $\beta$ -secretase).

© 2004 Elsevier Ltd. All rights reserved.

The proteolytic enzyme memapsin 2 ( $\beta$ -secretase, BACE-1) is one of two proteases that cleave the  $\beta$ -amyloid precursor protein (APP) to produce the 40–42 residue amyloid- $\beta$  peptide (A $\beta$ ) in the human brain, a key event in the progression of Alzheimer's disease (AD).<sup>1,2</sup> Because of its involvement in an early stage of the cascade of events leading to the pathogenesis of AD, inhibition of memapsin 2 has become an excellent target for AD.<sup>3–5</sup> We recently designed a number of potent memapsin 2 inhibitors incorporating a nonhydrolyzable Leu-Ala hydroxyethylene dipeptide isostere.<sup>6</sup> Potent memapsin 2 inhibitors incorporating other transition-state isosteres have also been reported recently.<sup>7</sup> Our first generation memapsin inhibitors were designed based upon memapsin 2 specificity studies.<sup>8</sup> One such inhibitor is OM99-2 (**1**), which has shown a  $K_i$  value of 1.6 nM for human memapsin 2.<sup>6a</sup> In order to obtain specific ligand-binding site interactions in the active site of memapsin 2, we subsequently determined the X-ray

crystal structure of **1**-bound memapsin 2 at 1.9 Å resolution<sup>9</sup> (Fig. 1).

This crystal structure provided important molecular insight, which may aid the design of novel and selective

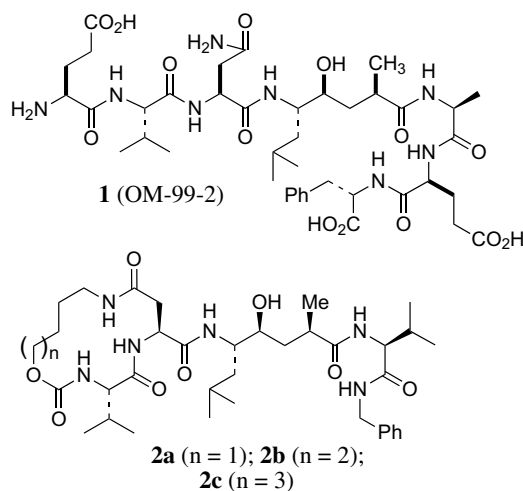


Figure 1.

**Keywords:** Alzheimer's disease; Inhibitor; Memapsin 2; Secretase.

\* Corresponding author. Tel.: +1 312 996 9672; fax: +1 312 996 1547; e-mail: [arungos@uic.edu](mailto:arungos@uic.edu)

inhibitors of memapsin 2. We are particularly intrigued by a number of key interactions involving P<sub>1</sub>–P<sub>4</sub> side chains in the S<sub>1</sub>–S<sub>4</sub> subsites.<sup>9</sup> It appears that the P<sub>1</sub>-Leu and the P<sub>3</sub>-Val fill the hydrophobic pocket effectively. Furthermore, the P<sub>2</sub>-Asn is involved in a hydrogen bond with Arg-235. Interestingly, the P<sub>4</sub>-Glu is hydrogen bonded to P<sub>2</sub>-Asn and possibly assists the formation of the P<sub>2</sub>-Asn hydrogen bond with Arg-235. Our preliminary modeling studies indicate that a suitably functionalized 15- or 16-membered cycloamide–urethane could effectively hydrogen bond with Arg-235 as well as effectively fill in the hydrophobic pockets in the S<sub>2</sub>–S<sub>4</sub> binding sites. Herein, we report our preliminary investigation that led to the design and synthesis of cycloamide–urethane-derived inhibitors of memapsin 2. Cyclic inhibitors containing a 16-membered ring turned out to be more potent than the acyclic counterpart. A 16-membered macrocycle containing a *trans*-olefin has shown the best memapsin 2 inhibitory potency with a K<sub>i</sub> value of 14 nM. Various cycloamide–urethanes were conveniently prepared by efficient ring-closing metathesis utilizing Grubbs' catalyst.<sup>10</sup>

As outlined in Figure 2, we planned to synthesize various macrocyclic inhibitors from the corresponding cyclic olefins **3a–c** by hydrogenation of the olefins followed by removal of the hydroxyl protecting group. Cyclic derivatives **3a–c** were obtained by coupling cyclic dipeptide acids **4a–c** and the amine derived from known dipeptide isostere **5**.<sup>6a</sup> Cyclic dipeptide acids **4a–c** can be derived

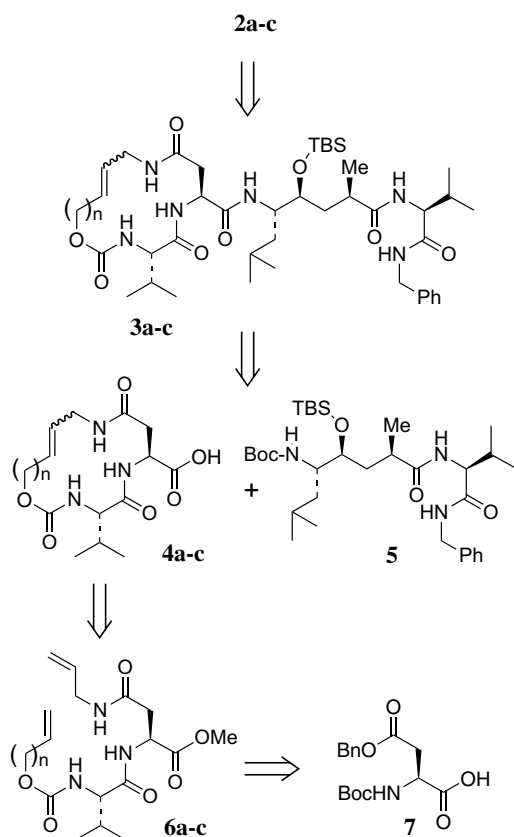
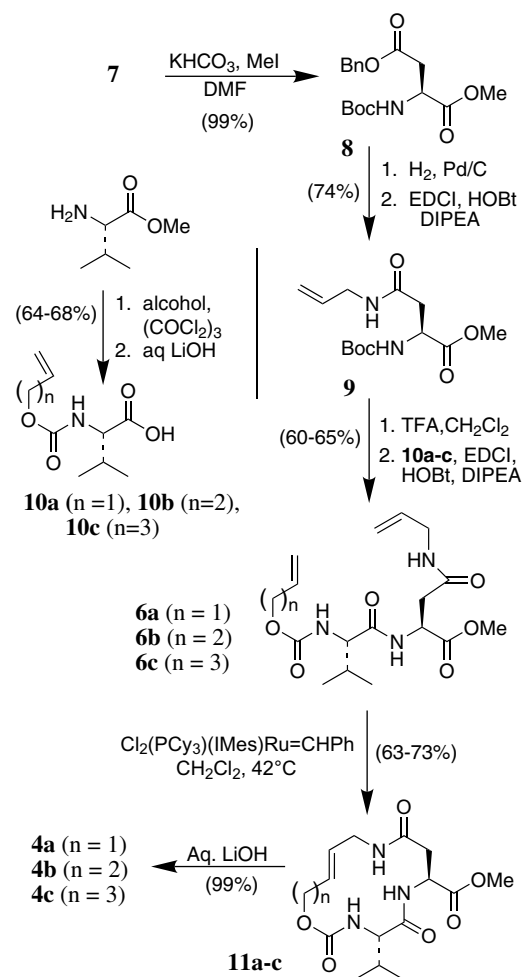


Figure 2.

by ring-closing olefin metathesis of acyclic terminal olefins **6a–c** followed by saponification of the resulting esters. Olefin metathesis was expected to provide a *cis/trans* mixture.<sup>11</sup> Various terminal olefins **6a–c** were synthesized from commercially available<sup>12</sup> *N*-(*tert*-butoxycarbonyl)-*L*-aspartic acid-4-benzylester **7**. We also planned to prepare the acyclic inhibitors by coupling of the **6a–c**-derived carboxylic acids and the corresponding amine derived from Leu-Ala dipeptide **5**. This enabled us to examine inhibitory potencies of various acyclic and cyclic inhibitors.

Synthesis of various cyclic carboxylic acid containing Val-Asn dipeptides **4a–c** is shown in Scheme 1. Treatment of known 4-benzylester **7** with KHCO<sub>3</sub> and methyl iodide in DMF for 65 h provided methyl ester **8** in near quantitative yield. Hydrogenolysis of the benzyl ester over 10% Pd–C, followed by coupling of the resulting acid with allylamine in the presence of 1-[3-(dimethylamino) propyl]-3-ethyl-carbodiimide hydrochloride (EDCI), diisopropylethylamine (DIPEA), and 1-hydroxybenzotriazole (HOBt) afforded allyl amide **9** in 74% yield for the two-step sequence. Synthesis of various urethanes **10a–c** was carried out with valine methyl ester by a one pot two-step procedure. Thus, a mixture of

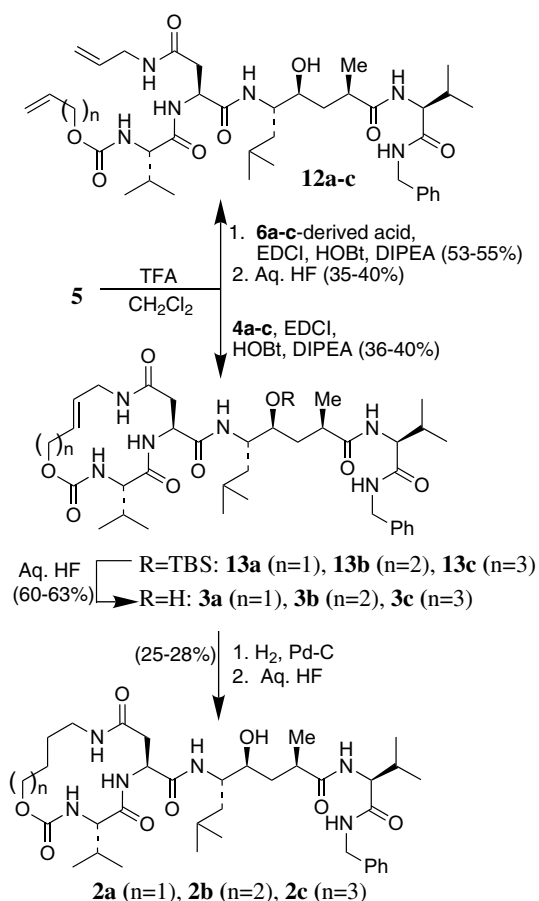


Scheme 1.

valine methyl ester hydrochloride and Hunig's base in  $\text{CH}_2\text{Cl}_2$  was slowly added to a solution of triphosgene in  $\text{CH}_2\text{Cl}_2$ . The resulting isocyanate was then reacted with allyl alcohol, 3-buten-1-ol, or 4-penten-1-ol for 24h to afford the corresponding urethanes.<sup>13</sup> Saponification of the methyl esters with aqueous lithium hydroxide furnished the valine derivatives **10a–c** (64–68% yield).

Exposure of **9** to trifluoroacetic acid (20% in  $\text{CH}_2\text{Cl}_2$ ) effected the removal of the Boc group. To the resulting TFA salt, Hunig's base was added to liberate the free amine. This was coupled with the valine derivatives **10a–c** under standard peptide coupling conditions (EDCI, HOBt, DIPEA) to afford olefins **6a–c** in 60–65% yield. Ring-closing metathesis of dienes **6a–c** proceeded smoothly in the presence of Grubbs' second generation catalyst<sup>14</sup> to afford macrocyclic *trans*-olefins as the major products in very good yields (63% for **11a**; 68% for **11b** and 73% for **11c**).<sup>15</sup> Saponification of **11a–c** with aqueous LiOH afforded the acids **4a–c** in near quantitative yields.

Synthesis of acyclic and cyclic inhibitors are shown in Scheme 2. Selective removal of the Boc-group from the known silyl ether **5** by treatment with trifluoroacetic acid (20% in  $\text{CH}_2\text{Cl}_2$ ) at 23°C for 30 min provided the corresponding amine. Coupling of the resulting amine with acids derived from aqueous LiOH promoted



Scheme 2.

Table 1. Structure and potencies of memapsin 2 inhibitors

Entry	Compound	$K_i$ (nM)
1		26.6
2		87.2
3		217.6
4		61.4
5		28.4
6		108.2
7		112.1
8		14.2
9		25.1

saponification of esters **6a–c** in the presence of EDCI and HOBt provided the corresponding coupled products in 53–55% yields. Removal of the silyl ether with aqueous HF in THF yielded the acyclic inhibitors **12a–c** in 35–40% yield. For synthesis of cyclic inhibitors, 5-derived amine was coupled with cyclic dipeptides **4a–c** as described above to afford the corresponding silyl ethers **13a–c** in modest yield (36–40%). Removal of the silyl ether furnished 14- to 16-membered mono-unsaturated macrocyclic inhibitors **3a–c** in a typical 60–63% yield. Macrocyclic 14- to 16-membered saturated inhibitors were prepared by catalytic hydrogenation of olefins **13a–c**, followed by deprotection of silyl ether with aqueous HF in THF to afford inhibitors **2a–c** in modest yields (25–28% for the two steps).

The inhibitory potencies of various acyclic and cyclic memapsin 2 inhibitors are shown in Table 1. Inhibitory potencies of various inhibitors against recombinant memapsin 2 were measured using our previously described assay protocol.<sup>16</sup> As can be seen, the size of the alkyl chains of the acyclic inhibitors is important for potency. Furthermore, ring size of the mono-unsaturated and saturated macrocyclic rings is critical to the observed inhibitory activities. Both mono-unsaturated and saturated 14-membered inhibitors (**3a** and **2a**) have shown significantly higher inhibitory potencies compared to acyclic inhibitor **12a**. It appears inhibitor **3b** with a 15-membered unsaturated ring is more suitable than the 14-membered inhibitor **3a**. As mentioned earlier, based upon the inhibitor-bound crystal structure, it appeared that a 16-membered ring with a P<sub>2</sub>-asparagine derivative could effectively interact with the Arg-235 residue as well as fill in the S<sub>2</sub>–S<sub>3</sub> sites. Indeed, the corresponding 16-membered mono-unsaturated and saturated inhibitors (**3c** and **2c**) are significantly more potent than their acyclic counterpart with respective K<sub>i</sub> values of 14 and 25 nM against memapsin 2.

To gain further insight into the molecular binding properties of inhibitors **2c** and **3c**, we attempted to resolve

the inhibitor-bound crystal structure of the protein–ligand complexes. This effort led to the determination of the three-dimensional structure of **2c**-bound memapsin 2 by X-ray diffraction at a resolution of 2.8 Å.<sup>17</sup> A stereoview of the inhibitor-bound structure is shown in Figure 3. As can be seen, the (*S*)-hydroxyl group of inhibitor **2c** hydrogen bonds with the catalytic aspartates (Asp-32 and Asp-228) of memapsin 2. The P<sub>1</sub>-isobutyl side chain and the P<sub>1</sub>'-methyl moieties of **2c** effectively fill in the S<sub>1</sub> and S<sub>1</sub>'-regions, respectively, in the enzyme active site. The P<sub>2</sub>'-inhibitor carbonyl hydrogen bonds with Tyr-198 at a distance of 2.41 Å. The binding properties of the P<sub>2</sub>-cycloamide–urethane is quite intriguing. While the valine side chain and the urethane side chain fill in the hydrophobic pocket effectively, the asparagine carbonyl of **2c** is within hydrogen bonding distance (2.56 Å between the heavy atoms) to the Arg-235 of the memapsin 2. In order to analyze the protein–ligand interactions in greater precision for further improvements of this class of inhibitor with structure-based design, higher resolution crystal structures will be attempted.

Memapsin 1 (BACE-2) is the closest homologous protease to memapsin 2. Some circumstantial evidence indicates that memapsin 1 is linked to the pathogenesis of Alzheimer's disease, but this has not been established conclusively.<sup>19</sup> If it is shown that memapsin 1 is not involved in the disease pathogenesis, then selectivity over memapsin 1 is desirable. Conversely, if involvement of memapsin 1 is proven, along with memapsin 2, it may be a therapeutic target. In any event, we have examined inhibitory properties of inhibitors **2c** and **3c** against memapsin 1 as well. Inhibitors **2c** and **3c** inhibited memapsin 1 with K<sub>i</sub> values of 4.5 and 31 nM, respectively. It appears that the *E*-olefin in inhibitor **3c** is responsible for its slight selectivity over memapsin 1. Interestingly, saturated inhibitor **2c** is 5-fold more potent for memapsin 1 than memapsin 2. This cross inhibition of memapsin 1 is not totally unexpected since memapsin 1 also cleaves the β-secretase site of APP

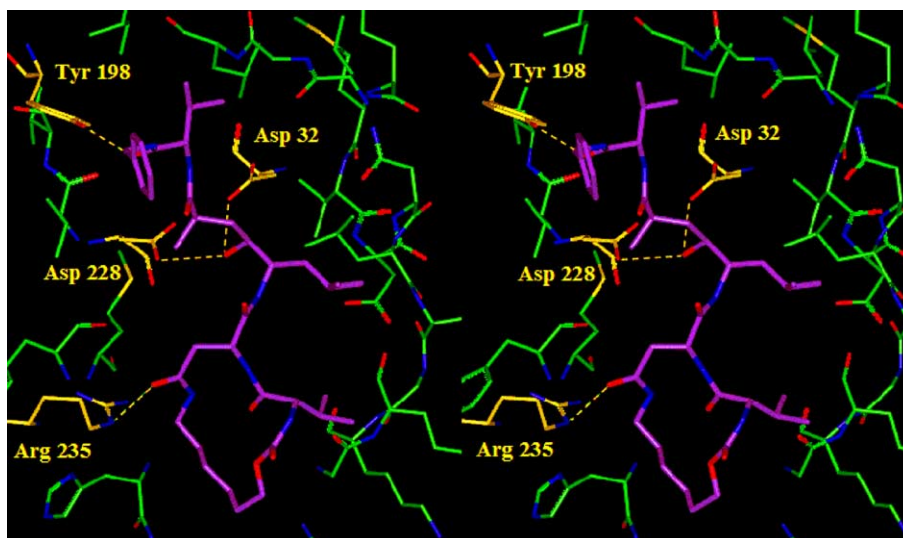


Figure 3. Inhibitor **2c** (magenta) bound X-ray crystal structure of memapsin 2.

and APP with Swedish mutations.<sup>20</sup> A structure-based design strategy may aid the design of inhibitors with enhanced selectivity over memapsin 1. We have also examined cellular inhibition of memapsin 2 by **2c** in Chinese hamster cells. It has shown an average cellular IC<sub>50</sub> value of  $3.9 \pm 1.2 \mu\text{M}$  ( $n = 2$ ) compared to IC<sub>50</sub> value of  $45 \pm 5 \mu\text{M}$  for OM-99-2 ( $K_i = 1.2 \text{ nM}$ ).<sup>21</sup>

In conclusion, structure-based design of cycloamide–urethane functionality at P<sub>2</sub>–P<sub>3</sub> resulted in a novel series of memapsin 2 inhibitors. These cyclic ligands are designed to allow effective hydrogen bonding with specific residues in the S<sub>2</sub>-active site. Interestingly, 16-membered mono-unsaturated and saturated inhibitors (**3c** and **2c**) are the most potent inhibitors. A preliminary inhibitor-bound memapsin 2 structure of **2c** indicated that the asparagine carbonyl of **2c** is within hydrogen bonding distance to the Arg-235 of memapsin 2. This interaction is apparent in the X-ray structure of OM-99-2-bound memapsin 2. Further investigations including specific nonpeptidic ligand design from these preliminary studies are currently underway.

#### Acknowledgements

Financial support by the National Institutes of Health (AG 18933) is gratefully acknowledged. J.T. is the holder of the J.G. Puterbaugh Chair in Biomedical Research at the Oklahoma Medical Research Foundation. The authors thank Mr. Debasis Manna for experimental assistance.

#### References and notes

- (a) Selkoe, D. J. *Nature* **1999**, *399A*, 23; (b) Selkoe, D. *Physiol. Rev.* **2001**, *81*, 741.
- Vassar, R.; Citron, M. *Neuron* **2000**, *27*, 419.
- (a) Roggo, A. *Curr. Top. Med. Chem.* **2002**, *2*, 359; (b) Olson, R. E.; Thompson, L. A. *Ann. Rep. Med. Chem.* **2000**, *35*, 31.
- Vassar, R.; Bennett, B. D.; Babu-Khan, S.; Kahn, S.; Mendiaz, E. A.; Denis, P.; Teplow, D. B.; Ross, S.; Amarante, P.; Loeloff, R.; Luo, Y.; Fisher, S.; Fuller, J.; Edenson, S.; Lile, J.; Jarosinski, M. A.; Biere, A. L.; Curran, E.; Burgess, T.; Louis, J. C.; Collins, F.; Treanor, J.; Rogers, G.; Citron, M. *Science* **1999**, *286*, 735.
- (a) Lin, X.; Koelsch, G.; Wu, S.; Downs, D.; Dashti, A.; Tang, J. *Proc. Natl. Acad. Sci. U.S.A.* **2000**, *97*, 1456; (b) Sinha, S.; Lieberburg, I. *Proc. Natl. Acad. Sci. U.S.A.* **1999**, *96*, 11049.
- (a) Ghosh, A. K.; Shin, D.; Downs, D.; Koelsch, G.; Lin, X.; Ermolieff, J.; Tang, J. *J. Med. Chem. Soc.* **2000**, *122*, 3522; (b) Ghosh, A. K.; Bilcer, G.; Harwood, C.; Kawahama, R.; Shin, D.; Downs, D.; Hussain, K. A.; Hong, L.; Loy, J. A.; Nguyen, C.; Koelsch, G.; Ermolieff, J.; Tang, J. *J. Med. Chem.* **2001**, *44*, 2865.
- (a) Shuto, D.; Kasai, S.; Kimura, T.; Liu, P.; Koushi, H.; Takashi, H.; Shibakawa, S.; Hayashi, Y.; Hattori, C.; Sazbo, B.; Isiura, S.; Kiso, Y. *Bioorg. Med. Chem. Lett.* **2003**, *13*, 4273; (b) Tung, J. S.; Davis, D. L.; Anderson, J. P.; Walker, D. E.; Mamo, S.; Jewett, N. E.; Hom, R. K.; Sinha, S. *J. Med. Chem.* **2002**, *45*, 259; (c) Hom, R. K.; Gailunas, A. F.; Mamo, S.; Fang, L. Y.; Tung, J. S.

- Walker, D. E.; Davis, D.; Thorsett, E. D.; Jewett, N. E.; Moon, J. B.; Varghese, J. *J. Med. Chem.* **2004**, *47*, 158.
- (a) Ermolieff, J.; Loy, J. A.; Koelsch, G.; Tang, J. *Biochemistry* **2000**, *39*, 12450; (b) Turner, R.; Koelsch, G.; Hong, L.; Castenheira, P.; Ghosh, A. K.; Tang, J. *Biochemistry* **2001**, *40*, 10001.
- Hong, L.; Koelsch, G.; Lin, X.; Wu, S.; Terzyan, S.; Ghosh, A. K.; Zhang, X. C.; Tang, J. *Science* **2000**, *290*, 150.
- Grubbs, R. H.; Chang, S. *Tetrahedron* **1998**, *54*, 4413.
- Ghosh, A. K.; Swanson, L. M.; Hussain, K. A.; Cho, H.; Walters, D. E.; Holland, L.; Buthod, J. *Bioorg. Med. Chem. Lett.* **2002**, *12*, 1993.
- Available from Aldrich Chemical Co., Milwaukee, WI.
- N,N'*-Disuccinimidyl carbonate promoted alkoxy carbonylation protocols also provided similar results, see: (a) Ghosh, A. K.; Duong, T. T.; McKee, S. P. *Tetrahedron Lett.* **1991**, *32*, 4251; (b) Ghosh, A. K.; Duong, T. T.; McKee, S. P.; Thompson, W. J. *Tetrahedron Lett.* **1992**, *33*, 2781.
- Chatterjee, A. K.; Morgan, J. P.; Scholl, M.; Grubbs, R. H. *J. Am. Chem. Soc.* **2000**, *122*, 3783, and references cited therein.
- Olefin metathesis typically provided a 4:1 mixture of *trans/cis* isomers for 14- to 16-membered rings. The *cis/trans* mixture has been separated by silica gel chromatography using 25% ethyl acetate and hexanes as the eluent. The olefin geometry of the major *trans*-isomers was established by extensive decoupling experiments. The coupling constants of the olefinic protons ( $J_{ab} = 15\text{--}16 \text{ Hz}$ ) indicated that the *trans*-cycloamides are formed.
- Memapsin 2 inhibition was measured using recombinant enzyme produced from *E. coli* expression as described in Ref. 5a. A fluorogenic substrate Arg-Glu (EDANS)-Glu-Val-Asn-Leu-Asp-Ala-Glu-Phe-Lys (Dabcy)-Arg was used with  $0.47 \mu\text{M}$  of the enzyme in 0.1M Na-acetate + 5% dimethylsulfoxide, pH4.5 at 37°C. The excitation wavelength was 350nm and the emission wavelength was 490nm. Details of this assay will be published in due course.
- The protein–ligand X-ray structure of **2c**-bound memapsin 2 has been deposited in PDB with the access code: 1XS7. Memapsin 2/inhibitor **2c** crystal was soaked in the mother liquor plus 20% (v/v) glycerol and quickly frozen under a cryogenic nitrogen gas stream. Diffraction data of a single crystal was recorded on a Mar 345 image plate mounted on a MSC-Rigaku RU-300 X-ray generator with Osmic focusing mirrors. Data were integrated and merged using previously described protocols.<sup>9,16</sup> The crystal form was determined to be monoclinic with a resolution of 2.8 Å. The unit cell parameters are  $a = 85.8$ ,  $b = 87.8$ ,  $c = 130.6$ ,  $\beta = 89.8^\circ$ . The structure was determined by molecular replacement implemented with the program AmoRe using the previously determined memapsin 2 structure (PDB ID: 1M4H) as a search model.<sup>18</sup> Rotation and translation functions followed by the rigid-body refinement with data from 15 to 3.5 Å resolution in space group  $P2_1$  gave unambiguous solutions for the four memapsin 2 molecules in the asymmetric unit. A random selection of 8% of reflections was set aside as the test set for cross-validation during the refinement. The refined model has well defined electron density for the inhibitor and its corresponding structure was built into the active site. The four molecules in the crystallographic asymmetric unit have essentially identical structures.
- Hong, L.; Turner, R. T., III; Koelsch, G.; Shin, D.; Ghosh, A. K.; Tang, J. *Biochemistry* **2002**, *41*, 10963.

19. Yan, R.; Bienkowski, M. J.; Shuck, M. E.; Miao, H.; Troy, M. C.; Pauley, A. M.; Brashier, J. R.; Stratman, N. C.; Mathewa, W. R.; Buhl, A. E.; Carter, D. B.; Tomasselli, A. G.; Parodi, L. A.; Heinrikson, R. L.; Gurney, M. E. *Nature* **1999**, *402*, 533.
20. (a) Bennett, B. D.; Babu-khan, S.; Loeloff, R.; Louis, J. C.; Curran, E.; Citron, M.; Vasser, R. *J. Biol. Chem.* **2000**, *275*, 20647; (b) Farzan, M.; Schnitzler, C. E.; Vasilieva, N.; Leung, D.; Choe, H. *Proc. Natl. Acad. Sci. U.S.A.* **2000**, *97*, 9712.
21. Cells transfected with the human APP Swedish mutation were cultured essentially as described previously.<sup>22</sup> Conditioned media was collected following a 24 h incubation with compound OM99-2 in 0.4% DMSO and assayed for A $\beta$ <sub>40</sub> by sandwich ELISA (BioSource International) for determination of IC<sub>50</sub>.
22. Chang, W. P.; Koelsch, G.; Wong, S.; Downs, D.; Da, H.; Weerasena, V.; Gordon, B.; Devasamudram, T.; Bilcer, G.; Ghosh, A. K.; Tang, J. *J. Neurochem.* **2004**, *89*, 1409.